Large Scale Testing of Ground Reaction for Design of Laterally Loaded Piles in the Shaftesbury Shale

Hossein Rafiei Renani & Garry Stevenson
Klohn Crippen Berger, Vancouver, British Columbia, Canada
Derek Martin
Klohn Crippen Berger (Seconded), Vancouver, British Columbia, Canada
Badr Benabdellah
SNC-Lavalin, Vancouver, British Columbia, Canada
Colin Dreger
SNC-Lavalin (Seconded), Vancouver, British Columbia, Canada
Dan Brown
Dan Brown and Associates, Knoxville, Tennessee, United States
Andrew Watson
BC Hydro, Vancouver, British Columbia, Canada

ABSTRACT
As part of the Site C hydroelectric project, bi-directional lateral load tests were carried out in two 2.6 m diameter drilled shafts to reliably determine the response of the Shaftesbury shale foundation at depth. Two 2.3 m diameter loading assemblies equipped with high capacity Osterberg load cells were concreted inside the shafts and were used to apply bi-directional horizontal loads of up to 81 MN to the shaft walls. For each test, seven inclinometers and eight displacement transducers were installed to record the displacements inside and around the shaft. The results of uniaxial compression tests and borehole pressuremeter tests were used to independently predict the ground response using analytical and empirical p-y models. This paper provides a description of these well-instrumented full-scale lateral load tests and compares the measured ground response with that predicted using the p-y models.

RÉSUMÉ
Dans le cadre du projet hydroélectrique Site C, des essais de chargement latéral bidirectionnel ont été effectués dans deux puits forés de 2.6 m de diamètre afin de déterminer de manière fiable la réponse, en profondeur, de la fondation rocheuse. La fondation rocheuse est principalement constituée de schiste de Shaftesbury. Deux assemblages de 2.3 m de diamètre équipés de cellules de charge à haute capacité de type Osterberg ont été bétonnés à l'intérieur des puits. Les deux assemblages ont été utilisés pour appliquer des charges horizontales bidirectionnelles allant jusqu'à 81 MN sur les parois des puits. Pour chaque essai, sept inclinomètres et huit capteurs de déplacement ont été installés pour enregistrer les déplacements à l'intérieur et autour du puits. Les résultats des essais de compression uniaxiale et des essais pressiométriques en forage ont été utilisés pour prédire indépendamment la réponse de la fondation à l'aide de modèles p-y analytiques et empiriques. Cet article fournit d'abord une description de ces essais de chargement latéral bien instrumentés et réalisés à grande échelle, et compare ensuite la réponse mesurée de la fondation à celle prédite à l'aide des modèles p-y.

1 INTRODUCTION

The Site C Clean Energy Project located 7 km southwest of Fort St. John, British Columbia is the third dam and hydroelectric generating station on the Peace River downstream of the W.A.C Bennet and Peace Canyon dams. It consists of a 60 m high main earthfill dam across the Peace River and six generating units with a total capacity of 1100 MW on the right bank of the river. Early site investigations and testing were conducted in the 1970's and 1980's. The Site C project received approval from the provincial government in 2014, construction started in 2015 and is ongoing.

The Site C project is founded on the Cretaceous rocks of the Shaftesbury formation which primarily consist of sub-horizontal layers of silty shale with interbeds of shale, siltstone, and sandstone. A stratigraphic column was developed by dividing the bedrock into fourteen rock units with those at higher elevations being generally of lower quality.

The main dam was designed as an earthfill dam with an impervious core to be constructed across the river, with the spillway and powerhouse structures located on the right (South) bank. Lower quality rock near the surface of the right abutment was excavated and replaced with roller-compacted concrete (RCC) buttresses extending down to elevation 375 m to create a sound foundation for the overlying spillway and powerhouse structures (Heidstra et al. 2017). A watertight approach channel was designed to convey water from the reservoir upstream of the earthfill dam toward the powerhouse intakes and spillway headworks. More details on the geological conditions, site investigations, and design of the Site C project is given by Watson et al. (2019). The general arrangement of the project is shown in Figure 1.

Additional foundation enhancement measures were designed for the right bank to boost reliability, robustness, and resilience over the 100-year design life of the project. This included the design of large diameter shear piles with lengths of up to 46 m to connect the RCC buttresses to the bedrock at depth.

This study presents the results of laboratory tests, borehole pressuremeter tests, and two full-scale lateral load tests performed in drilled shafts which were used to establish the ground reaction response for design and optimization of the shear piles at Site C. The results of tests are compared with those obtained from analytical and empirical lateral load-displacement (p-y) models.

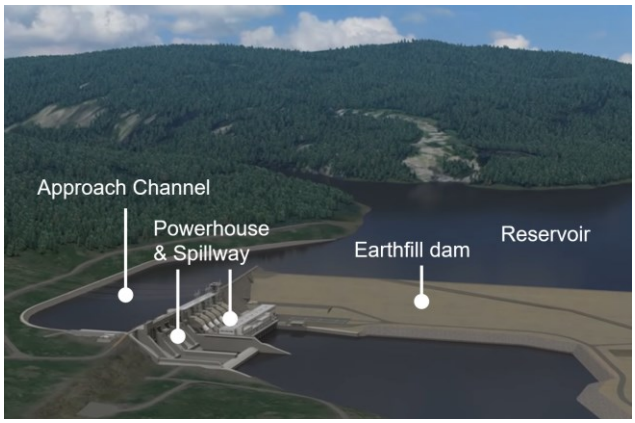

Figure 1. General arrangement of the Site C project

2 RECENT SITE INVESTIGATIONS

The early stiffness and strength tests for characterization of the right bank foundation were primarily focused on rock units above the river valley which had weakened and softened. Additional testing was performed in 2020 to quantify the increasing stiffness and strength of the foundation with depth down to elevation 340 m.

A series of unconfined compression tests was conducted on 61 mm diameter samples of intact rock according to ASTM D7012. Table 1 shows a summary of the values of uniaxial compressive strength, UCS, and Young's modulus, E, measured perpendicular to bedding from 16 tests on the samples of silty shale between elevations 369 m and 375 m.

In order to measure the in-situ stiffness of silty shale at depth, pressuremeter tests were performed using 96 mm diameter high pressure dilatometer (HPD) in the same holes from which the unconfined compression test samples were obtained. The results of 19 pressuremeter tests conducted between elevations 369 m and 375 m are also shown in Table 1.

It can be observed that the mean value of Young's modulus measured parallel to bedding using the in-situ pressuremeter tests is three times higher than that obtained from the laboratory unconfined compression tests perpendicular to bedding. This is thought to be related to the horizontally bedded structure of the rock, lack of confinement in the laboratory tests compared to the in-situ borehole measurements, and the disturbance experienced by the laboratory samples during coring, handling, and sample preparation for testing despite following best practices.

The laboratory compression and in-situ pressuremeter tests provided invaluable information regarding the stiffness and strength of the rock at small scale. However, it is well-established that rock mass behavior is influenced by scale effects. As the volume of rock under investigation increases, it contains more cracks, joints, and other defects which can lead to a reduction in the overall strength and stiffness properties. Numerous studies have documented this trend and proposed empirical upscaling relations to estimate the mechanical properties at large scale (e.g., Bieniawski 1978; Heuze 1980; Hoek and Brown 1980; Hoek and Diederichs 2006). However, these upscaling relations are predominantly based on data from strong rocks with UCS values typically greater than 50 MPa. Hence, applicability of these empirical upscaling relations to the type of shale at Site C was highly uncertain. Because of the importance and scale of this project, large-scale tests were performed to directly measure the response of the ground at the scale of the shear piles considered for the right bank foundation enhancements.

Table 1. Properties of silty shale at depth measured perpendicular and parallel to bedding

Property	Test	Mean	Standard deviation
Perpendicular to bedding			
UCS (MPa)	Unconfined compression	16.9	4.8
E (GPa)	Unconfined compression	3.7	1.5
Parallel to bedding			
E (GPa)	Pressuremeter	11.2	2.7

3 OVERVIEW OF LATERAL LOAD TESTS

A common method for testing of laterally-loaded piles is given in ASTM D3966, which involves pushing the pile head against a reaction system at the surface, and measuring pile head deflections. This test mimics the ground-pile interaction in high-rise buildings, bridges, offshore structures, and other typical applications where horizontal seismic inertia, wind, wave, and impact loads are primarily applied to the pile head and a wedge of soil or rock surrounding the deflected length of the pile deforms towards the ground surface. This mode of pile loading and ground deformation near surface was not representative of the mechanism of ground-pile interaction at depth anticipated for the shear piles at Site C.

Bi-directional lateral load tests are well suited for applications where ground response to lateral loads at depth is of interest. In this method, a test shaft is drilled and a loading assembly with horizontally expanding load cells is installed in the shaft at the depth of interest. The load cells are used to apply bi-directional lateral loads to the

shaft wall while the resulting displacements are measured using displacement transducers and inclinometers. This test can be used to directly determine the lateral ground reaction (p-y) curve, and some examples are given by O'Neill et al. (1997), Brown and Camp (2002), and Brown et al. (2010). Considering the representative mechanisms of loading and deformation at depth, this type of test was chosen for determining the ground response to lateral loads at Site C.

4 FULL-SCALE BI-DIRECTIONAL LATERAL LOAD TESTS AT SITE C

Two 2.6 m diameter shafts were drilled in the spillway stilling basins from elevation 396 m to a depth of 43 m. To minimize excavation-induced disturbance to rock surrounding the shafts, percussion tools were not employed during drilling and a rotary drilling rig was used with a core barrel and drilling bucket. High resolution downhole video cameras were used to capture the geological features exposed on the shaft walls. The rock mass was found to be massive and free from major joints at the scale of the shafts. This was consistent with the cores obtained from nearby pressuremeter holes where rock quality designation, RQD, was close to 100. In addition, SoniCaliper surveys were conducted in the drilled shafts to obtain the as-built 3D geometry of the shafts.

Two 2.3 m diameter loading assemblies were designed and fabricated to apply large bi-directional horizontal loads to the shaft walls (Figure 2). The loading assemblies were lifted and positioned in Shafts 1 and 2 with their centers at elevations 374 and 370 m (depths of 22 and 26 m below grade), respectively. Subsequently, they were cast in concrete with maximum aggregate size of 10 mm and minimum compressive strength of 35 MPa at 7 days.

Each loading assembly was equipped with two Osterberg cells (O-cells) providing a total rated loading capacity of 53.4 MN (26.7 MN by each O-cell). The active segment of the loading assembly was 2.0 m high and could be pushed out by the expansion of the O-cells against the 4.0 m high passive side of the assembly. Teflon sheets were placed on the contact surfaces above and below the active segment to minimize frictional resistance against its sliding. Eight linear vibrating wire displacement transducers (LVWDTs) were attached to the bearing plates on the active and passive sides of the O-cells to measure the expansion at the center of each shaft. For a rigid loading system, the expansion at the center is equal to the sum of lateral displacements in the active and passive sides of the shaft wall. In addition to the LVWDTs, two in-place inclinometers were installed on the passive side of each loading assembly to measure displacements towards the passive side. Hence, displacements towards the active side could be calculated by subtracting displacements on passive side from O-cell expansions.

In addition to the LVWDTs and inclinometers inside the shafts, five shape acceleration arrays (SAAs) were installed around each shaft to monitor the distribution of displacements in the surrounding rock mass and to add redundancy to the measurement system. The arrangement of the instruments is shown in Figure 2.

The bi-directional lateral load tests produced average lateral pressures onto the 2.6 m wide by 2.0 m high rock surface in contact with the active segment which reached 14.0 and 15.5 MPa in Shafts 1 and 2, respectively. These pressures approached the average UCS value of intact rock measured in the laboratory. Loads were applied at a typical rate of 0.5 MN per minute with four one-hour hold periods at loads of 10, 20, 30, and 40 MN and two unload-reload cycles at 10 and 40 MN load levels.

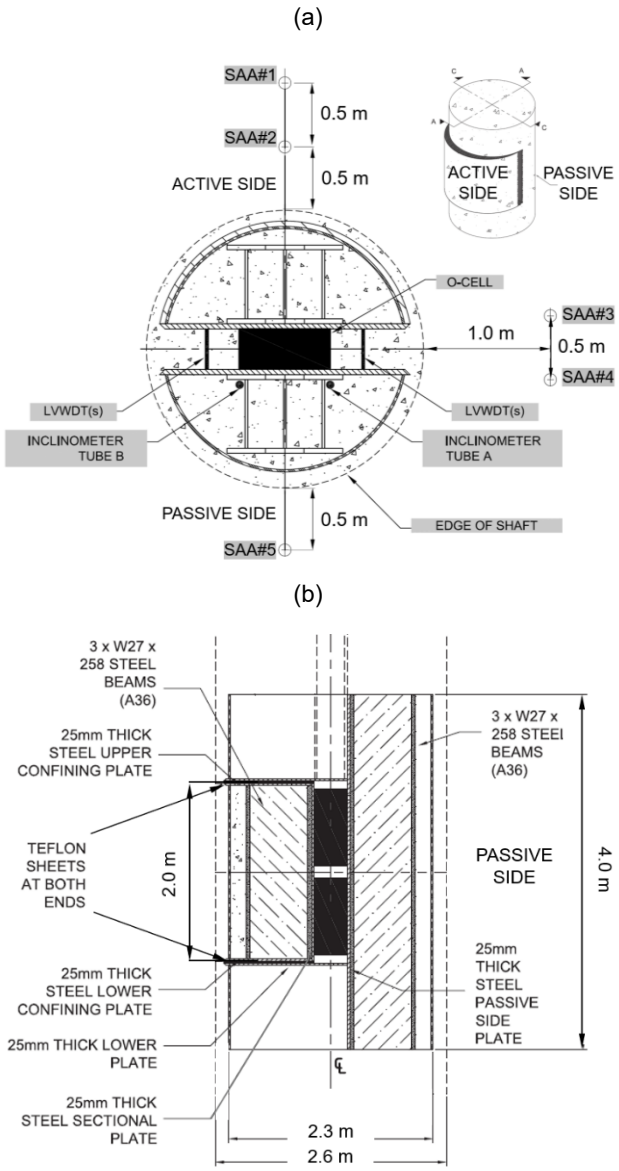

Figure 2. Configuration of the loading assembly and instrumentation, a) plan view, b) vertical cross section

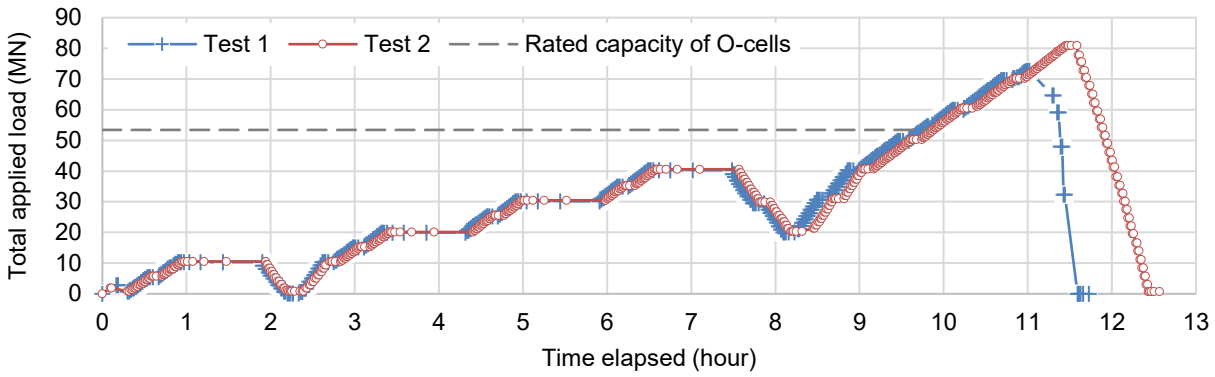

Figure 3. Loading procedure in the bi-directional lateral load tests

Figure 3 shows the loading procedure followed in Tests 1 and 2 which were performed in Shafts 1 and 2, respectively. The loading in Tests 1 and 2 followed a similar trend and reached the 53.4 MN rated capacity of the O-cell assemblies after about ten hours. Since O-cells typically have significant reserve capacity, loading was continued beyond the rated capacity to maximize the information obtained from the tests. Test 1 was completed after about eleven and a half hours with a maximum applied load of 72.74 MN, and Test 2 took about twelve and a half hours with a maximum applied load of 80.95 MN. The load-displacement response of the rock was very similar in the two tests. For brevity, the results of Test 2 are presented in this study.

Even under such high applied pressures, the magnitude of recorded displacements remained less than 1.5 mm, indicating a stiff and strong rock mass response. Figure 4 shows the results of measurements inside the shaft in Test 2 including the maximum displacements at the center of the passive side and average displacements across the 4 m height of the passive side obtained from the in-place inclinometers. Clean data and reasonable trends were obtained from displacement measurements on the passive side. Figure 4 also shows the average displacements across the 2 m height of the active side obtained by subtracting the average displacements on the passive side from the average expansions recorded by the LVWDTs. Calculated displacements on the active side showed abnormal trends due to insufficient accuracy of the LVWDTs at such small displacement levels.

The SAAs installed around the shafts provided precise and accurate measurements of displacements which supplemented those recorded inside the shafts. Figure 5 shows rock mass displacements at the center elevation of the loading assembly in Test 2 recorded by SAA#1 and SAA#2 on the active side at distances of 1.0 m and 0.5 m from the shaft wall, respectively. As expected, reasonable load-displacement trends were observed with higher displacements recorded closer to the loading assembly. Of particular importance was the observation that displacements were largely reversible after unloading indicating an essentially elastic response of the rock mass under the large applied loads. The energy loss in the load-unload cycle is likely to be primarily dissipated by the breakage of bonds and friction on the interfaces between rock, concrete, and steel.

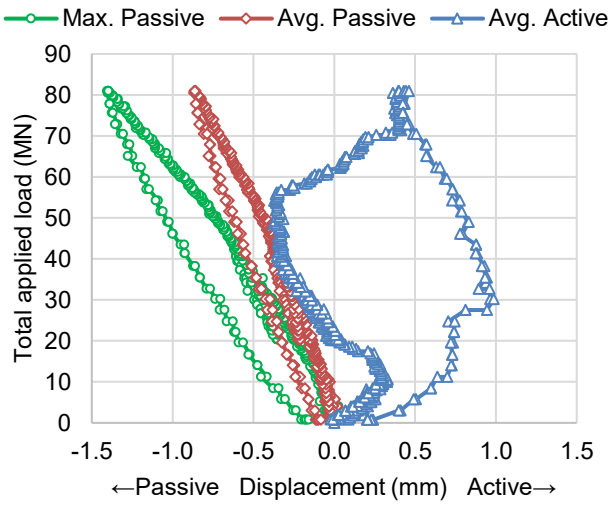

Figure 4. Displacements inside the shaft during Test 2

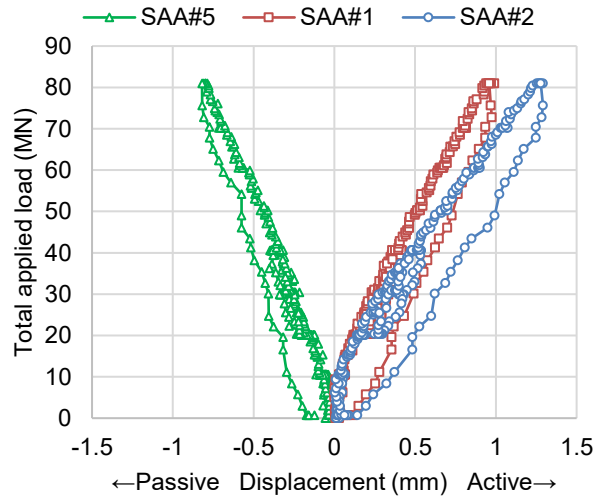

Figure 5. Displacements in the rock during Test 2

Figure 6 shows the displacement profiles during Test 2 recorded by SAA#1 and SAA#2 on the active side and SAA#5 on the passive side. The maximum displacements and concentration of displacements around the center elevation of the loading assembly were highest for SAA#2 followed by SAA#1 and SAA#5. This pattern is consistent with the proximity of these SAAs to the shaft wall as well as the heights of active segment and passive side of the loading assembly. The displacements recorded by SAA# 3 and SAA#4 located on the tensile side of the shaft were less than 0.2 mm at maximum load and recovered after unloading. Since highest displacements were recorded by SAA#1 and SAA#2 on the active side of the loading assembly where largest stresses were applied to the rock, the measurements of these instruments are primarily analyzed in this study.

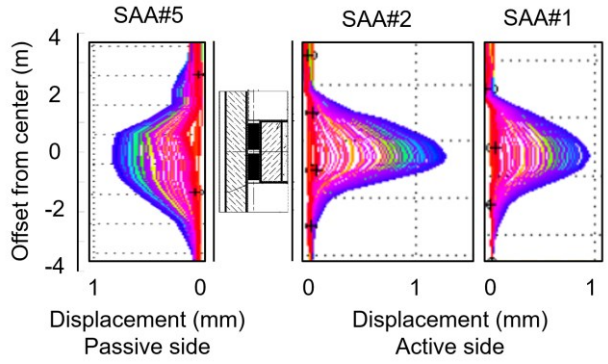

Figure 6. Displacement profiles in the rock during Test 2

5 PREDICTIONS OF GROUND REACTION MODELS

Engineering design of laterally loaded piles is commonly based on ground-pile interaction analyses in which the pile is represented as a beam in contact with a series of springs representing ground reaction. In this approach, ground response to lateral loads at each elevation is specified by a p-y curve for the spring where p is the lateral load per unit length of the pile and y is the lateral displacement. There are many available p-y models for various materials to estimate the in-situ ground response from available strength and stiffness properties. The following p-y models were used prior to performing the lateral load tests to obtain unbiased predictions of ground reaction response.

The elastic solution for expansion of a cylindrical cavity under uniform internal pressure was used to obtain an approximate p-y curve:

$$\Delta\sigma_r = 2E\Delta u_r/[B(1+\nu)] \quad [1]$$

where $\Delta\sigma_r$ and Δu_r are the changes in internal pressure and radial displacement on the cavity wall, B is the cavity diameter, E and ν are the Young's modulus and Poisson's ratio of the surrounding material, respectively. Input parameters including B=2.6 m, average E=11.2 GPa obtained from the pressuremeter tests and ν=0.3 were used for the rock.

The analytical solution for deflection of a beam on elastic subgrade obtained by Vesic (1961) provided another p-y model:

$$p = 0.65y[E/(1-\nu^2)]\left[(EB^4)/(E_pI_p)\right]^{1/12} \quad [2]$$

where p is the lateral load per unit length of the shaft, y is the lateral displacement, E_p and I_p are the Young's modulus and moment of inertia of the pile, respectively. In addition to the elastic constants mentioned above for the rock, E_p=35 GPa was used for the pile, and I_p was calculated for the 2.6 m diameter cross section of the shaft.

Reese (1997) proposed an empirical p-y curve for weak rocks which is also recommended by Brown et al. (2018) and is commonly used in practice. For depths greater than three times the shaft diameter, as was the case for the lateral load tests at Site C, the model gives:

$$p = 500Ey \quad for \quad y \le y_A \quad [3]$$

$$p = (p_{ur}/2)(y/y_{rm})^{0.25} \quad for \quad y_A < y < 16y_{rm} \quad [4]$$

$$p = p_{ur} \quad for \quad y \ge 16y_{rm} \quad [5]$$

with

$$y_{rm} = k_{rm}B \quad [6]$$

$$p_{ur} = 5.2\alpha_r q_{ur} B \quad [7]$$

$$y_A = [p_{ur}/(1000Ey_{rm}^{0.25})]^{1.333} \quad [8]$$

$$\alpha_r = 1 - (2/3)(RQD/100) \quad [9]$$

where p_{ur} is the ultimate resistance per unit length of the shaft at depths greater than three times the shaft diameter, q_{ur} is the compressive strength of the rock, RQD is the rock quality designation, and k_{rm} is a constant ranging from 0.0005 to 0.00005. For this model, average q_{ur}=16.9 MPa from the unconfined compression tests, average E=11.2 GPa from the pressuremeter tests, RQD=100 from cores logs, and k_{rm}=0.0005 were used.

Reese et al. (2004) proposed an empirical p-y curve for strong rocks which can be given by:

$$p = 1000yq_{ur} \quad for \quad y < y_1 \quad [10]$$

$$p = (950y_1 + 50y)q_{ur} \quad for \quad y_1 \le y \le 6y_1 \quad [11]$$

with

$$y_1 = 0.0004B \quad [12]$$

For this model, average q_{ur}=16.9 MPa from the unconfined compression tests was used.

More recently, Liang et al. (2009) adopted a hyperbolic p-y model for massive rock masses given by:

$$p = y/[(1/K_i) + (y/p_{ur})] \quad [13]$$

with

$$K_i = E(B/B_{ref})exp(-2v)\left[(E_pI_p)/(EB^4)\right]^{0.284} \quad [14]$$

$$p_{ur} = \left(\frac{\pi}{4}\sigma_1' + \frac{2}{3}\tau_{max} - p_a\right)B \quad [15]$$

$$\tau_{max} = 0.45\sigma_{ci}^{0.5} \quad [16]$$

where p_{ur} is the ultimate resistance per unit length of the shaft at great depth, τ_{max} is the maximum horizontal shear resistance of the rock-pile interface, σ_{ci} is the unconfined compressive strength of intact rock, p_a is the active horizontal earth pressure if present, and B_{ref} is the reference shaft diameter equal to 0.305 m. Stresses in Equation 16 must be specified in terms of MPa. Rock mass strength, σ_1', is obtained from the empirical failure criterion proposed by Hoek and Brown (1980, 2019):

$$\sigma_1' = \sigma_3' + \sigma_{ci}\left(m_b\frac{\sigma_3'}{\sigma_{ci}} + s\right)^a \quad [17]$$

with

$$m_b = m_i\, exp\left(\frac{GSI-100}{28-14D}\right) \quad [18]$$

$$s = exp\left(\frac{GSI-100}{9-3D}\right) \quad [19]$$

$$a = \frac{1}{2} + \frac{1}{6}\left[exp\left(\frac{-GSI}{15}\right) - exp\left(\frac{-20}{3}\right)\right] \quad [20]$$

where σ_1' is the major effective principal stress at failure, σ_3' is the minor effective principal stress considered in this model to be equal to the vertical effective overburden stress at the depth of interest, m_i is a constant which depends on the type of rock, GSI is the geological strength index, and D is the disturbance factor which depends on the excavation method. The interested reader is referred to Rafiei Renani and Cai (2022) who provided a comprehensive review of the Hoek–Brown failure criterion for rock masses.

For this p-y model, rock mass parameters including E=11.2 GPa, σ_{ci}=16.9 MPa, m_i=6 for shale as recommended by Hoek and Marinos (2000), GSI=100 for the massive structure of the rock mass, and D=0 for rotary drilling with core barrel were used. This set of GSI and D values give upper bound strength values for the rock mass.

Figure 7 shows the ground reaction curves predicted by the p-y models using the same set of stiffness and strength properties obtained from the laboratory and pressuremeter tests. Displacements recorded by SAA#2 closest to the active segment of the loading assembly during Test 2 are also shown in Figure 7 for comparison.

It can be observed that the predictions of various analytical and empirical p-y models vary considerably indicating a high degree of prediction uncertainty. The empirical model by Reese (1997) provided the best estimate of peak displacement at maximum load. However, the slope of this p-y curve at maximum test load is significantly lower than the slope of experimental data, and decreases further at higher loads leading to an overestimation of displacements at such loads. The second closest p-y curve was obtained from the elastic solution for expansion of a cylindrical cavity under uniform internal pressure. This model overestimated the measured peak displacement by a factor of two. The third closest p-y curve was based on the solution of Vesic (1961) for deflection of a beam on elastic subgrade. This p-y curve overestimated the measured peak displacement by a factor of four. The p-y model of Liang et al. (2009) overestimated the displacement at maximum load by an order of magnitude. This is because the model underestimated the ultimate load bearing capacity of the rock mass at depth even though undisturbed and fracture-free conditions (GSI=100, D=0) were considered for the rock mass. The poorest results were obtained from the p-y model of Reese et al. (2004) which predicted the ultimate load bearing capacity of the rock mass to be about one-half of the maximum load applied during the lateral load tests.

The elastic solution for cylindrical cavity expansion was used to estimate a representative in-situ rock mass modulus by fitting the measured displacements (Figure 7). A Young's modulus of 20 GPa provided a good match to the measured displacement at maximum load. This value of modulus was consistent with that obtained from three-dimensional numerical modeling of the tests presented in a companion paper (Dreger et al. 2022).

The ground response measured during the large-scale lateral load tests was crucial in minimizing uncertainties in ground-pile interaction analyses which were used to optimize the design of the shear piles while satisfying serviceability and strength limit states for the piles and surrounding rock mass.

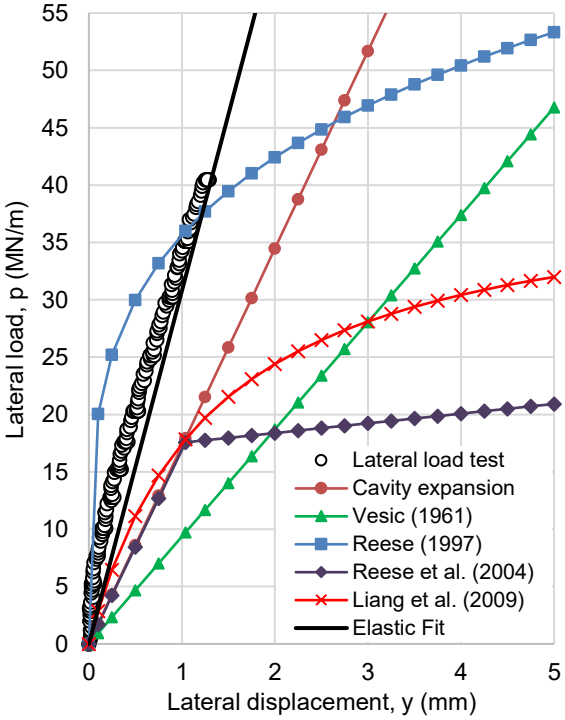

Figure 7. Comparison of predicted, measured, and matched ground reaction curves

6 DISCUSSION

The Young's modulus of 20 GPa obtained from the large-scale lateral load tests was much higher than the mean values of 3.7 and 11.2 GPa obtained from small-scale laboratory and pressurmeter tests, respectively (Table 1). This could be due to the lower degree of disturbance to the rock in the full-scale tests in terms of both the severity of disturbance and relative volume of damaged rock compared to the total volume of rock under aplied loads. In addition, small cracks and defects which may dominate the response of small-scale samples were less impactfull when testing a massive rock mass at large scale.

The pressuremeter tests were performed at certain elevation intervals inside boreholes which were open above and below the testing interval. Under the applied pressuremeter loads, the rock could deform towards these open areas of the boreholes. However, the shafts for the lateral load tests were completely filled with concrete before starting the tests. Hence, deformation of the rock from the loaded area towards the areas above and below the loading assembly was met with additional resistance from the concrete infill leading to a higher degree of effective confinement and therefore a stiffer overall response. Finally, the flowable concrete used for infilling the test shafts had the additional benefit of filling small voids and cracks in the rock mass near the shaft wall, and this may have also contributed to the stiffer response. Considering the minimum disturbance and favorable performance of the rock mass during the tests, the drilling and backfilling procedures for the test shafts were adopted for construction of the shear piles.

7 CONCLUSIONS

Design of shear piles at Site C required reliable information regarding the in-situ response of the silty shale rock mass to large lateral loads at depth. Small-scale laboratory uniaxial compression tests and borehole pressuremeter tests provided useful information for preliminary design.

Two bi-directional lateral load tests were performed in 2.6 m diameter test shafts to determine the rock mass response at large scale. For each test, a 2.3 m diameter loading assembly equipped with two Osterberg-cells with a combined rated capacity of 53.4 MN was positioned at the desired depth and the shaft was fully backfilled with concrete. An extensive array of inclinometers and displacement transducers was used to monitor displacements inside and outside the shafts as the O-cells were pressurized to apply loads to the shaft walls. Maximum total loads of 72.74 and 80.95 MN were applied in the tests and maximum measured displacements remained below 1.5 mm. The SAAs installed outside the shafts and the in-place inclinometers installed inside the shafts provided reliable displacement measurements. However, the LVWDTs installed between the loading plates to measure the expansion of the O-cells did not provide usable information due to lack of sufficient accuracy at such small displacement levels. The measured load-displacement response was similar in both tests and the deformations were largely reversible upon unloading implying a stiff and strong rock mass.

The ground reaction curve obtained from the tests was compared with the analytical and empirical p-y curves predicted prior to performing the tests. The empirical model of Reese (1997) for weak rocks provided the closest estimate of displacement at maximum test load but significantly overestimated the degree of nonlinearity of the p-y response. While the relatively linear trend of experimental data was more similar to those obtained from the elastic solution for expansion of a cylindrical cavity under internal pressure and analytical solution of Vesic (1961) for deflection of a beam on elastic subgrade, they overestimated the magnitude of maximum displacement by factors of about two and four, respectively. The p-y model of Reese et al. (2004) for strong rock and that of Liang et al. (2009) for massive rock drastically overestimated the displacements at large applied loads due to underestimation of lateral load bearing capacity of the rock mass in these models.

The value of Young's modulus back-calculated from the full-scale lateral load tests was significantly higher than the average values obtained from the laboratory uniaxial compression and borehole pressuremeter tests. This was explained in terms of sample disturbance, effects of small cracks and defects, levels of confinement, and the positive effects of backfilling the test shafts with concrete. The full-scale tests provided essential and reliable information regarding the in-situ response of the rock mass to large lateral loads.

ACKNOWLEDGEMENTS

The authors would like to thank BC Hydro for sponsoring the large-scale lateral load tests and for permission to publish the results. Contributions of engineers from Klohn Crippen Berger, SNC-Lavalin, BC Hydro, Fugro Loadtest, RST Instruments, Aecon, Flatiron, Dragados, and EBC to the successful performance of the tests are acknowledged.

REFERENCES

Bieniawski, Z.T. 1978. Determining Rock Mass Deformability: Experience from Case Histories, *International Journal of Rock Mechanics and Mining Science & Geomechanics Abstracts*, 15: 237–247.

Brown, D. and Camp, W.M. 2002. Lateral Load Testing Program for the Cooper River Bridge, Charleston, SC. *Proceedings of the International Deep Foundations Congress 2002*, Orlando, Florida, Geotechnical Special Publication No. 116, 1: 95–109.

Brown, D.A., Turner J.T. and Castelli, R. J. 2010. *Drilled Shafts: Construction Procedures and LRFD Design Methods*. Geotechnical Engineering Circular No. 10, Report No. FHWA NHI-10-016. Washington, D.C.: U.S. Department of Transportation, Federal Highway Administration.

Brown, D.A., Turner J.T., Castelli, R. J. and Loehr, E.J. 2018. *Drilled shafts: Construction Procedures and Design Methods*. Geotechnical Engineering Circular

No. 10, Report No. FHWA NHI-18-024. Washington, D.C.: U.S. Department of Transportation, Federal Highway Administration.

Dreger, C., Nguyen, V., Martin, D., Rafiei Renani, H., Stevenson, G. and Watson, A. 2022. Large-scale Stiffness Tests Bounding a Deep Bedding Plane in the Shaftsbury Shales. *Proceedings of the 75th Canadian Geotechnical Conference: GeoCalgary 2022*, Calgary, Alberta.

Heidstra, N., Nunn, J., Watson, A., Dodman, K., Carter, R. and Burmeister, L. 2017. Roller Compacted Concrete Buttress at the Site C Clean Energy Project. *Canadian Dam Association Bulletin*, pp. 12–23.

Heuze, F. 1980. Scale Effects in the Determination of Rock Mass Strength and Deformability. *Rock Mechanics,* 12: 167–192.

Hoek, E. and Brown, E.T. 1980. *Underground Excavations in Rock*. Institution of Mining and Metallurgy, London.

Hoek, E. and Brown, E.T. 2019. The Hoek–Brown Failure Criterion and GSI–2018 Edition. *Journal of Rock Mechanics and Geotechnical Engineering*, 11: 445–463.

Hoek, E. and Diederichs, M.S. 2006. Empirical Estimation of Rock Mass Modulus. *International Journal of Rock Mechanics and Mining Science,* 43: 203–215.

Hoek, E. and Marinos, P. 2000. Predicting Tunnel Squeezing Problems in Weak Heterogeneous Rock Masses. *Tunnels and Tunnelling International*, 132: 45–51.

Liang, L., Yang, K. and Nusairat, J. 2009. P-Y Criterion for Rock Mass. *Journal of Geotechnical and Geoenvironmental Engineering,* 135 (1): 26–36.

O'Neill, M.W., Brown, D.A., Townsend, F.C. and Abar, N. 1997. Innovative Load Testing of Deep Foundations, *Transportation Research Record: Journal of the Transportation Research Board*, 1569: 17–25.

Rafiei Renani, H. and Cai, M. 2022. Forty-Year Review of the Hoek–Brown Failure Criterion for Jointed Rock Masses. *Rock Mechanics and Rock Engineering*, 55: 439–461.

Reese, L.C. 1997. Analysis of Laterally Loaded Piles in Weak Rock. *Journal of Geotechnical and Geoenvironmental Engineering*, 123 (11): 1010–1017.

Reese, L.C., Wang, S.T., Isenhower, W.M. and Arrellaga, J.A. 2004. *LPILE- A Program for the Analysis of Piles and Drilled Shafts under Lateral Loads*. Technical Manual, Ensoft, Inc., Austin, Texas.

Vesic, A.S. 1961. Beam on Elastic Subgrade and the Winkler Hypothesis. *Proceedings of the 5th International Conference on Soil Mechanics and Foundation Engineering*, 1: 845–850.

Watson, A.D., Stevenson, G.W. and Hanna A. 2019. Site C Clean Energy Project, Design Overview, *Proceedings of the 87th Annual Meeting of International Commission on Large Dams, Sustainable and Safe Dams Around the World*, 2019 Canadian Dam Association, Ottawa, Ontario, 2: 2574–2587.